Chapter 1

The normal child: growth and development of the infant and child; frequent and important normal variants

Karl Schneider

General remarks on the development of the human body

The body proportions and the size of the organs vary greatly in different age groups from birth to adolescence. In early life, 0–1 years of age, the head is very large, the neck extremely short and the trunk is long with a relatively short chest in relation to the abdomen (Figure 1.1). On the other hand, the arms and legs are relatively short in the first years. During the growth spurt, which starts at about eight years, the long bones of the extremities lengthen considerably, the neck becomes longer and the head smaller. The technician and the radiologist have to consider these extreme differences of body proportions for patients of different age groups. For example, if the radiographer does not collimate the exposure field for a chest radiograph closely in small premature babies, a cumulative high eye lens dose can result as a deterministic radiation effect. Of course, correct coning is also important at the lower field edge of a chest X-ray, because a great number of abdominal organs are exposed to radiation. Figure 1.2 shows the increase of optimally coned field size in radiographs of the chest and abdomen. A similar problem exists in multidetector CT of the chest in young children. This effect is called over ranging and must be kept as low as possible in small patients.

Concurrently with the changes of the body proportions there is a shift of the red bone marrow from the head and the long bones in infants to the axial skeleton (spine, pelvic bones, ribs and sternum) in older children. This process is nearly completed at about 15 years of age (Figure 1.3). Of note, Cristy *et al.* described bone marrow conversion, but did not mention the extramedullary hematopoiesis within the liver, spleen and the kidneys in the first three months. The distribution of red and yellow bone marrow is readily apparent on magnetic resonance (MR) images. The most significant changes occur in the long bones. In newborns the long bones of the arms and the legs are entirely filled with red marrow. After infancy the yellow marrow begins to extend from the center of the bone to the metaphyseal ends. The conversion of fatty marrow occurs earlier in the epiphyses and diaphyses than in the metaphyses. The partly converted normal marrow in children aged 10 years or older appears isointense or hyperintense to skeletal muscle on plain T1-weighted MR images, while focal neoplasms appear hypointense. In adults, only small areas of hematopoietic bone marrow persist in the vertebrae as well as proximal metaphyses of the femur and humerus.

Skull

Ossification of the skull (calvaria and skull base) starts prenatally at the 12th week. The ossification at the skull base is of the enchondral type, in the cranial vault of the desmal type. The synchrondroses at the base of the skull are widely open at birth. This growing cartilage of the synchrondroses at the skull base is relatively soft and can accidentally be passed by tubes and catheters. The cranial vault grows along the sutures depending on the intracranial pressure. The infant's head has six physiological gaps, so-called fontanels, which diminish in size gradually during the first 12 months. The great (anterior) fontanel between the frontal and parietal bones is the largest. It closes normally between 8 and 24 months. The posterior fontanel is very small and lies between the parietal bones and occipital bone. In most term neonates it is closed. The lateral fontanels are anterior and posterior to the squamous bones. All fontanels allow access to perform ultrasound of the brain and to perform Doppler examinations of intracranial vessels.

In infants there is great variation in the head shape: one example is a long skull with a large anterior–posterior (ap) diameter; and the opposite, a short head with large bitemporal diameter. The neurocranium in the first two years is considerably larger than the viscerocranium. In term infants the ratio is 4 to 1 and will reduce to a value of 2.5 at five years. The cranial sutures begin to close at the age of about seven years. Complete closure is noted in adulthood, between 30 and 40 years.

Wormian bones represent normal variants in skull growth, and are apparent as small bones located in and between normal sutures, frequently in the Lambda and Mendoza sutures. If abundant, Wormian bones may indicate an

Essentials of Pediatric Radiology, ed. Heike E. Daldrup-Link and Charles A. Gooding. Published by Cambridge University Press.

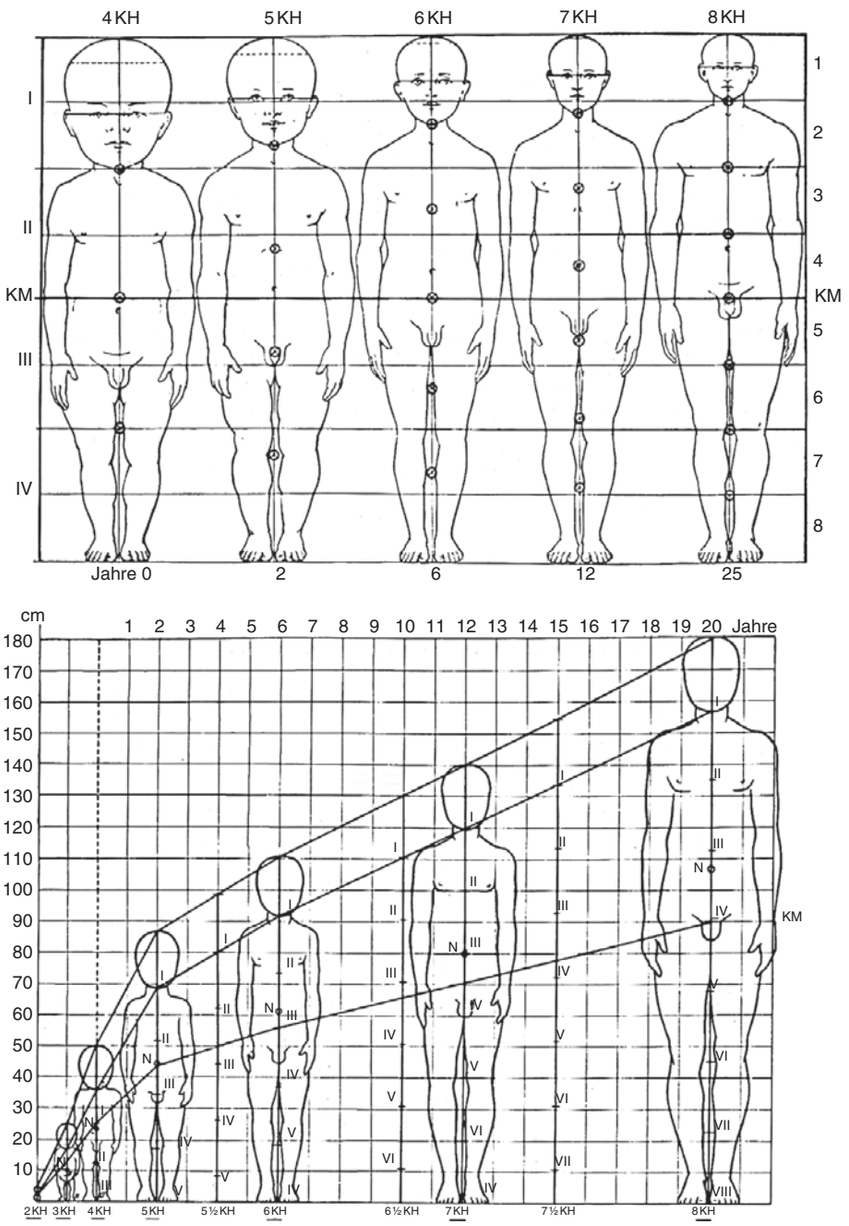

Figure 1.1 Body proportions during growth from newborn to adult. Illustration modified from *Handbuch der Anatomie des Kindes*, Bergmann Verlag München, 1938. KM (*Körper Mitte*) = body center; KH (*Kopfhöhe*) = length of the head. Body length can be calculated from KH; it is equivalent to 4 KH for a newborn and 8 KH for an adult.

osteogenesis imperfecta or cleidocranial dysplasia. A large extra bone located between the occipital and the parietal bones has been named "Inca bone." Sometimes, it is difficult to discern the sutures in skull radiographs, especially if the sutures are partially fused. In such cases, CT can be very helpful (Figure 1.4). Premature closure of the sutures occurs shortly after birth, or even prenatally, and is associated with typical abnormalities of the head shape, e.g. trigonocephaly or scaphocephaly. Convolutional markings (impressiones digitatae) may be seen in later childhood, mainly in school children. These striking findings in skull films are *not related* to an increased intracranial pressure, but are presumably caused by the pulsation effects of cortical arteries. Convolutional markings must be differentiated from the lacunar skull in patients with myelomeningocele and Arnold-Chiari II malformation, which is always present at birth. Other modeling effects on the tabula interna can be caused by Pacchioni granulations, parietal sinus and diploe veins. They are all harmless and need no further diagnostic work-up. Occasionally, a prominent protuberantia occipitalis externa must be distinguished from an occipital horn.

The development of facial bones and the orbits is greatly influenced by the development of the paranasal sinuses and the dentogenesis. The ethmoid cells and the antrum of the

mastoid bone are already developed in newborns. Other parts of the paranasal sinuses develop at the same time from very tiny cavities to large mucosa-lined structures, starting with the maxillary sinuses at the age of about two years and the sphenoidal sinus at four to five years. The frontal sinus starts its development at the age of eight years, and the mastoid cells pneumatize fully with puberty. There are two main deviations of the normal process of pneumatization of the facial bones and the skull base: hypo- and hyperpneumatization (Figure 1.5). The teeth in the maxilla and mandible are visible at birth. Dentition normally starts at the age of six months; the first permanent molar tooth erupts at seven years of age.

Brain

Many anatomical details of the developing brain can be imaged with US and MR. MR provides more-detailed information because the contrast resolution is better than with US. Diffusion-weighted imaging and tractography are very sensitive for the detection of brain edema and can differentiate it further. Finally, the arteries and veins can be depicted with magnetic resonance angiography. On the contrary, pulsed-wave (PW) US can not only demonstrate very fine cerebral vessels (Figure 1.6), but also provide hemodynamic information of cerebral blood flow.

Figure 1.2 Optimal field size of radiographs of the chest ap and the abdomen ap from the newborn to 15 years of age. The dashed line represents calculations from body weight and height using the Lindskoug model (Lindskoug, 1992).

The development of the brain can be easily followed in premature babies with high frequency sonography looking at the appearances of specific gyri and sulci. Also, the size and shape of the lateral ventricles and extracerebral spaces filled with cerebrospinal fluid (CSF) are evaluated. There are four sonographic criteria to follow normal brain development (Figure 1.7):

1. The brain surface before the 26th week is totally smooth with no sulci and widely open insular regions of the temporal lobes.
2. The first gyrus which can be seen at the 28th week is the gyrus cinguli.
3. The operculation of the temporal lobes is nearly completed in the 34th week.
4. At the 40th week, the brain has developed further with many sulci and the gyri at the surface. The brain completely fills the intracranial space at that time.

In addition, deeper cerebral structures, e.g. the basal ganglia, can be imaged with US. Especially, the caudate nucleus is very well suited for evaluation of the deep brain parts. Before the 32nd week, the head of the caudate nucleus is very echogenic, more than the adjacent internal capsule and the thalami. After the 34th week, the echogenicity of the head of the caudate nucleus has totally reversed. In very small premature babies, the external CSF spaces are wide; to a lesser extent also the ventricular system.

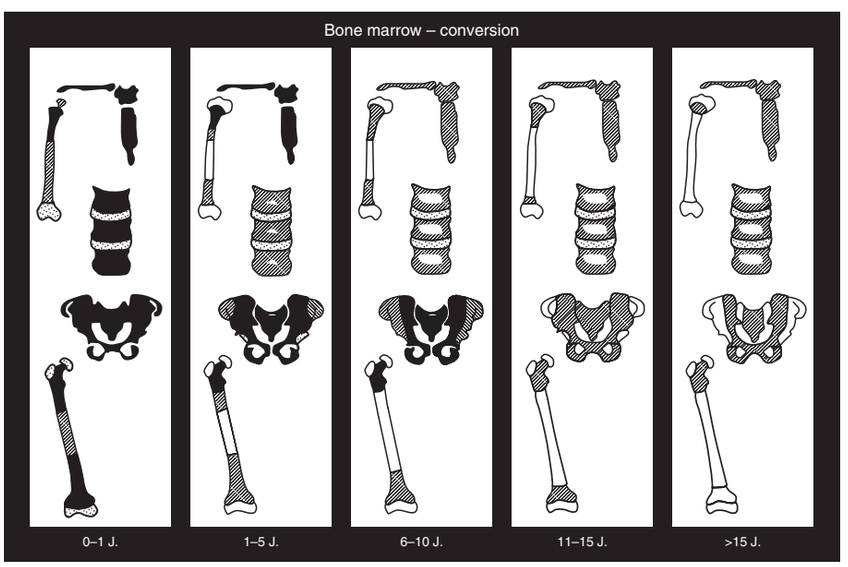

Figure 1.3 Age- and anatomic-site-dependent conversion from hematopoietic (black) to fatty (white) bone marrow (Kricun, 1985).

(A)

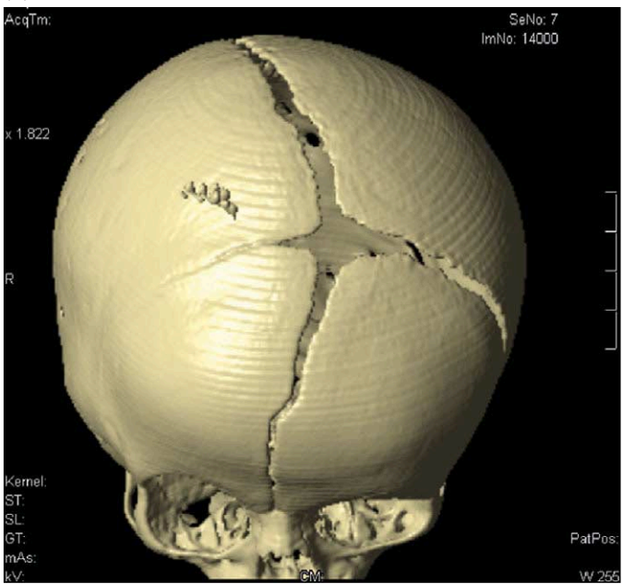

(B)

Figure 1.4 Unilateral synostosis of the right coronal suture clearly seen on (A) 3D-CT (bird's-eye perspective); (B) (right lateral aspect).

Figure 1.5 Missing pneumatization of the left mastoid process in a normal child.

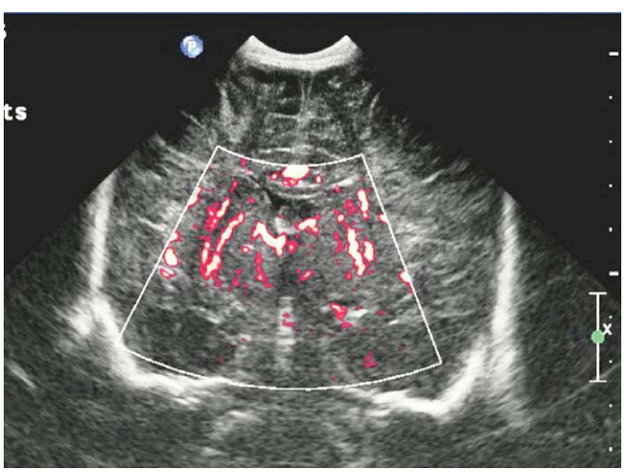

Figure 1.6 Prominent arteriae lenticulostriatae in a newborn brain visualized with power Doppler.

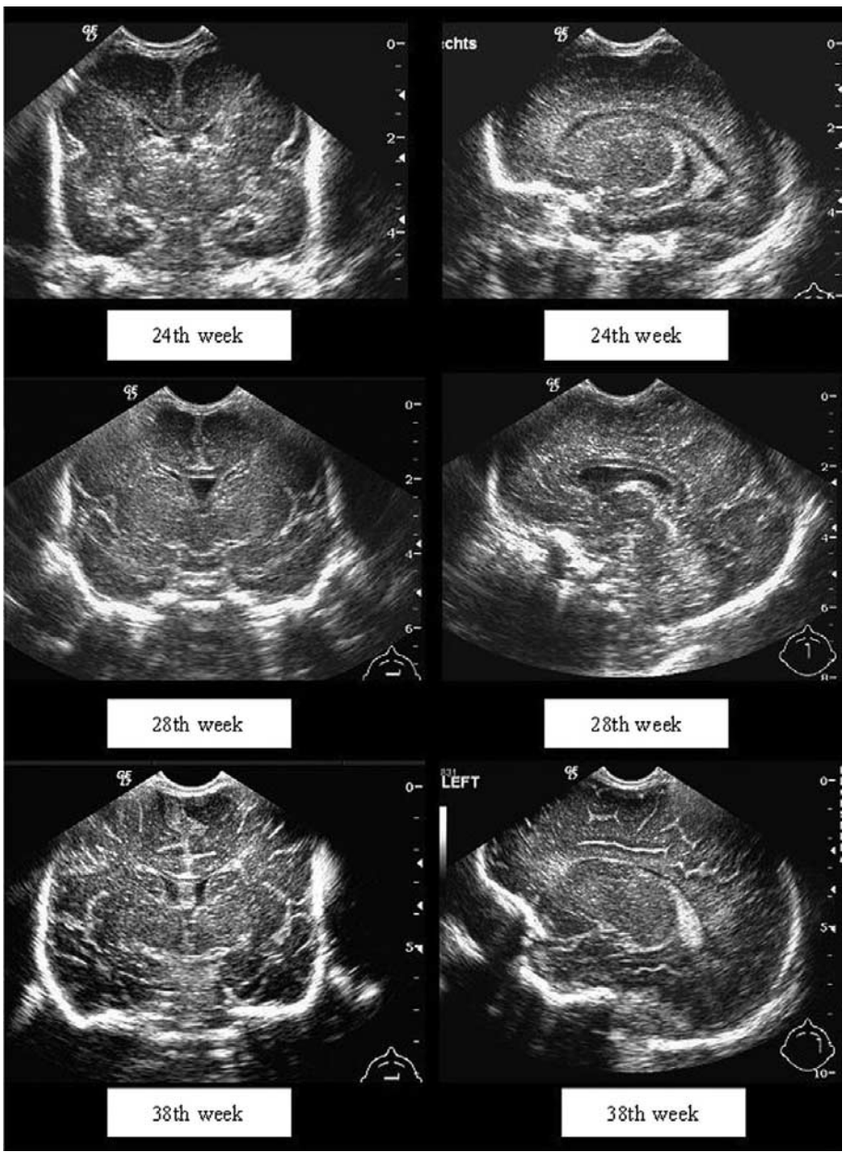

Figure 1.7 Brain development in premature babies illustrated in mid-coronal and parasagittal sections from extremely premature to mature babies.

There are many publications dealing with measurements of the size of the ventricular system, parenchymal thickness and the width of the extracerebral CSF space. A very simple measurement and a comparable value for all cross-sectional-imaging methods is the transverse diameter of the third ventricle. In all pediatric age groups the upper normal value for the third ventricle is 4.5 mm in horizontal and/or coronal sections.

A normal variant is the persistence of the cavum septi pellucidi. In premature babies the cavum vergae and the cavum septi pellucidi gradually regress. Most term babies have a septum with disappearance of the cavum. Other normal variants are: ventricular bands; tiny plexus cysts; round, or otherwise funny looking choroidal plexus. Beyond eight years, small intracranial calcifications can be detected in the falx, choroidal plexus, and the pineal gland on skull X-rays or on CT exams.

In addition to US, the myelination of the brain can be evaluated by a thorough analysis of MR images. At birth, the myelination is sparse and can be seen in the pons, pedunculi cerebelli, vermis, and the posterior crus of the internal capsule and very subtly in the gyrus praecentralis. A graph with a timetable shows the myelination in Figure 1.8. The myelination has progressed to the corpus callosum and the centrum semiovale in the eight-month-old infant. In addition, the myelin will then extend to the splenium, frontal and occipital lobes. This is the final progress of the myelination and is also called "arborization." MR is the optimal method to follow the development of sulci and gyri.

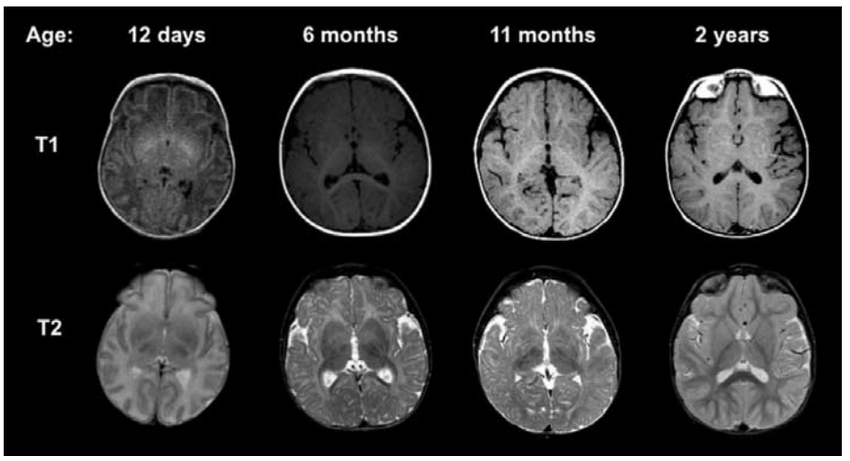

Figure 1.8 Normal appearance of the brain on T1- and T2-weighted MR images for children of different ages. The MR signal of white and gray matter shows an inversion from birth to 2 years of age. Myelination of the white matter during the first 6 to 8 months of life is best apparent on T1-weighted images, and myelination between 6 and 24 months of life is best evaluated on T2-weighted images. The myelination progresses with increasing age from caudal to cephalad and from dorsal to ventral.

PW-Doppler US can provide flow curves from specific blood vessels (cerebral arteries, cerebral veins, dural sinus). These curves represent a spectral distribution of different velocities sampled in the investigated vessel. Two measurements of velocity curves are of practical importance: peak systolic velocity (*S*), and end-diastolic velocity (*D*) of the Vmax curve. Using these two values, the resistive index can be calculated as $(S - D)/S$. Deeg *et al.* reported normal values of blood flow velocities and resistive indices of the main cerebral arteries for different age groups. The resistive indices are considerably higher in the first six months than in older children. In neonatal intensive care medicine, the Doppler examination of the anterior cerebral artery is a quick and simple method to detect hemodynamic effects on the cerebral circulation, e.g. caused by large left-to-right shunts such as a wide-open patent ductus arteriosus (PDA).

Table 1.1 Comparison of scan length of chest CT in pediatric patients of different age and size. Measurements of 275 spiral CT examinations

	Mean values ± 2 SD of scan length for chest CT (cm)		
Age group	Galanski *et al.*, 2005/2006[a]	Theocharopoulos *et al.*, 2007	Munich, 2007[b]
Newborn	10.1	8	11.0 ± 1.7
1 year	12.3	11	15.4 ± 4.4
5 years	16.4	15	17.9 ± 2.2
10 years	20.4	20	22.7 ± 3.2
15 years	26.0	24.3	28.0 ± 2.2
Adult	31.0	27	30.0 ± 2.0

Notes:
[a] Galanski *et al.*, 2007.
[b] Unpublished data.

Airways and chest

The diameters and the lengths of the chest change remarkably during development from the newborn to the child and adolescent. The shape of the newborn chest is at first a relatively short cylinder with a similar ap and lateral diameter. Beginning with the second year of life, the chest enlarges in the longitudinal direction (apicobasal) due to growth of the lungs (Table 1.1); later also in the transverse plane, and more in the horizontal than in the sagittal direction. In teenagers, the chest transverse diameter will have increased by a factor of two compared to the ap diameter (Figure 1.9).

The air-filled trachea is composed of two parts: a flexible cervical, and a nearly fixed thoracic part. Depending on the height of the diaphragm/respiratory phase, the intrathoracic part of the trachea slightly deviates to the right side. This effect is more evident in expiration (Figure 1.10). The reason is that, on the left side, two great arterial vessels (aortic arch and left pulmonary artery (PA)) cross the left main stem bronchus. This deviation is called tracheal scoliosis (old-fashioned, but more appropriate, is the term "bayonet shape"). It is a simple sign of the presence of a normal left-sided aortic arch. The normal trachea does not collapse completely. In patients with tracheomalacia, the trachea collapses completely on expiration. This can be due to a deficiency in the cartilaginous rings (primary tracheomalacia) or extrinsic compression (secondary tracheomalacia).

Infants normally have a large thymus which often increases further in size up to the age of two years. As the thymus can partially overlie the right and left heart border and can obscure the heart on chest X-rays, the term cardio-thymic shadow can be used. The shape of the thymus can vary greatly. If the thymus imitates a sail, this is called the sail or spinnaker sign. The thymus often has a cervical portion which is located behind the manubrium sterni and can move from the retrosternal position into the suprasternal fossa. The diagnosis of

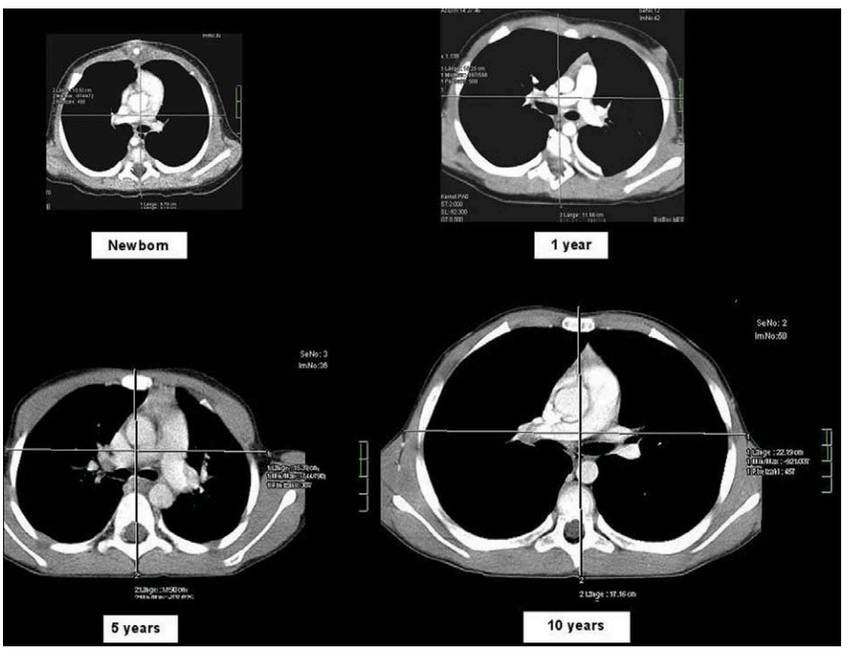

Figure 1.9 Axial CT sections through the level of the tracheal bifurcation are shown using the same magnification for patients of different ages.

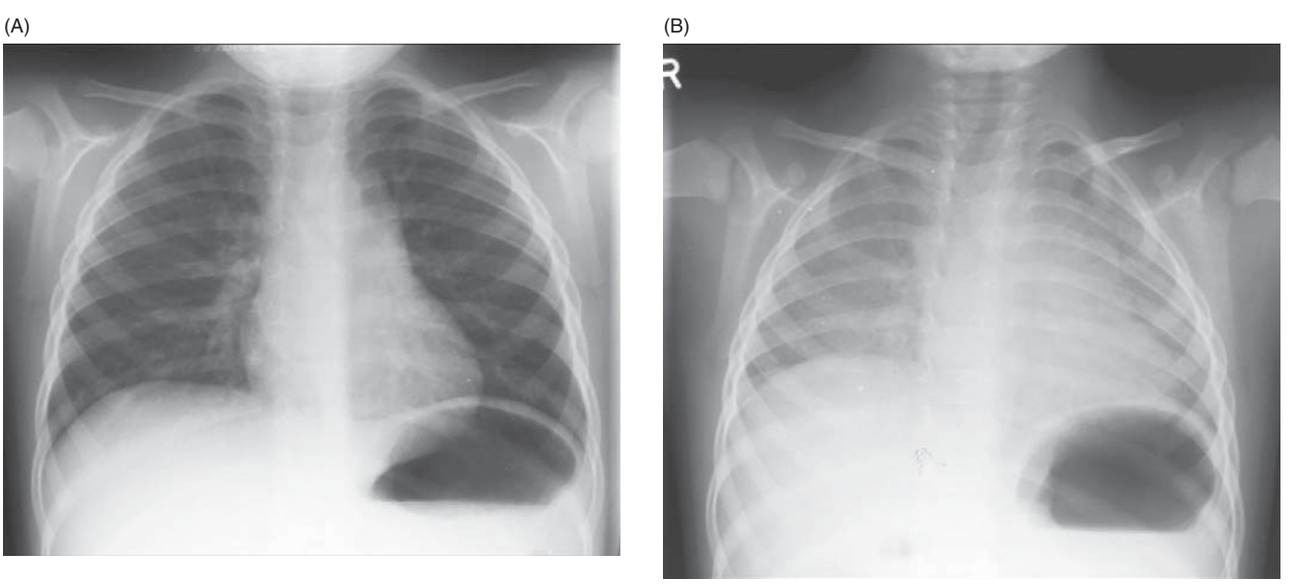

Figure 1.10 Chest pa X-rays of a two-year-old child in inspiration (A) and expiration (B). Variability of the shape of the trachea, heart and thymus size is clearly demonstrated.

thymus tissue is possible with US or MR. The normal cervical extension of a normal thymus must be differentiated from an ectopic cervical thymus, which appears as a cervical mass, which is discontinuous with the orthotopic thymus in the mediastinum and can be mistaken for a tumor or enlarged lymph node. The size of the thymus greatly depends on the respiratory phase, i.e. from the inflation of the lungs. In expiration the thymus is wide; in inspiration much smaller (Figure 1.10). After severe stress and in patients with severe and/or chronic diseases, the normal thymus decreases dramatically within a few days. Following chemotherapy, the thymus can show a "rebound" phenomenon with markedly increased size. Homogeneous texture, lack of mass effect on adjacent mediastinal vessels and flexible movement with inspiration and expiration on US can help to differentiate normal thymus from mediastinal masses.

The size of the heart can be measured using the cardiac index method. In newborns, the cardio-thoracic index is larger (up to 0.7) than in later childhood (0.5). There are some transitional effects related to incomplete expansion of the chest, less inflation of the lungs, open fetal shunts and high blood volume. In older infants, the use of the cardio-thoracic index requires a correct ap (anterior–posterior) or pa (posterior–anterior) projection of the chest radiograph, which very often is not achievable in young patients less than five years of age. Thus, a diagnosis of a cardiomegaly may be difficult in young children. In an unclear clinical situation we recommend an echocardiography.

In the first days after birth the mediastinum may be enlarged. In premature babies with an open ductus arteriosus, a prominent "ductus bump" may be seen at the aortic arch. The permanent closure of the ductus does not occur before the 12th week after birth. In older children, the area of the closed ductus appears in the aortopulmonic window as a ligament, which may be calcified and should not be mistaken for a calcified lymph node.

The lateral pleural recesses in young children are much deeper than in older children or young adolescents. In infants, the diaphragm can descend considerably in inspiration with completely flat contours on lateral chest films. The anterior recesses are not developed at this age. This explains why diaphragmatic borders are not well visible on inspiratory ap chest X-rays of young infants. Concurrently with the increase in length of the chest cage, these pleural recesses deepen considerably. These changes finally lead to the formation of the diaphragmatic dome.

The trachea and the bronchi (main, lobar and segmental bronchi) have relatively large diameters compared to the small peripheral bronchi. These anatomical findings are more marked in smaller children. This is the explanation of why in neonates a very prominent air bronchogram is visible even with normal lungs. Even more pronounced is the difference between the central and peripheral pulmonary arteries in the first three months. The reason for this finding is the high resistance of the small pulmonary arteries. These arterioles still have thick muscle walls persisting for a few months after birth, i.e. physiological transitory pulmonary hypertension. Therefore, following a transitional "wet-lung" syndrome, the lungs of young babies may show very few and small lung vessels. In addition, the interstitial lung tissue in early age is more prominent, which leads to an increased lung density compared to older children. Premature babies and, to a lesser proportion, term neonates can have hazy opacifications of the lungs on chest X-rays. In some cases there is an increase in pulmonary water as a transient phenomenon of immature lungs. But this finding may also be related to the predominantly lying position in the first months and the insufficient expansion of the chest by the respiratory muscles. Therefore, it is not surprising that the density of the lung parenchyma of infants and children of less than five years is higher in CT compared to older children and adolescents. The development of the human lung with all alveoli and capillaries continues throughout early childhood until approximately the age of eight years.

The degree of inflation of the lungs and the size of pulmonary vessels in young children is mainly influenced by external factors. Extreme crying or high fever without bronchopulmonary infection can simulate or even cause marked lung hyperemia and simulate a left-to-right shunt. In some cases, deep inspiratory effort can look like severe air-trapping and simulate bronchiolitis or asthma. If the inspiration is shallow, the normal prominent interstitium in infants can be mistaken for an interstitial lung disease. In small patients, especially in the first year, rotation of the chest can simulate an overinflation of a lung or even a pneumothorax. In neonates, skinfolds can be misdiagnosed as a pneumothorax. Critical analysis of the radiographs will lead to the right diagnosis in most cases.

Anomalies of the thoracic skeleton are relatively frequent. We often see fork ribs, which can simulate a rib tumor, but are harmless. Synchrondroses between the first and second rib are also occasionally seen. Abnormally shaped/shortened claviculae or scapulae are pathological findings and associated with certain syndromes, such as the VACTERL syndrome or certain skeletal dysplasias, such as very rare acamptomelic camptomelic dysplasias or cleidocranial dysplasias etc. Anomalies of the vertebra, e.g. butterfly vertebra, hemivertebra and more complex malformations are important markers for a hidden pathology, e.g. neurenteric cyst, esophageal duplication and Alagille syndrome.

Neck

Uncomplicated separation of the airway and feeding path in the middle of the pharynx requires a normal morphology of the epiglottis, larynx and esophagus. In addition, a normal swallowing process must coordinate the closure of the larynx, opening of the upper esophageal sphincter and the timely constriction of the lower pharyngeal muscles. Some newborns have transient coordination problems which may lead to aspirations of feedings (Figure 1.11); other newborns may have isolated or additional pharyngo-nasal reflux because of velopalatine insufficiency. These coordination problems often disappear within a few days. Lateral neck radiographs may show prominent prevertebral soft tissues, which show a decreasing thickness with increasing age. As a "rule of thumb," in infants between two and five years of age, the retrotracheal soft tissues should have approximately the thickness of the C5 vertebral body, and the retropharyngeal soft tissues should have approximately the thickness of 0.5 × C5. Between the ages of two to eight years the adenoids can be very large, obstructing the nasopharynx. If tracheal stenosis is suspected, evaluation of the airways with CT has replaced tracheal radiographs with a high kV technique. N. T. Griscom has published normal values of tracheal cross-sectional areas measured with CT.

Gastrointestinal tract

A "barium swallow" (we prefer low-osmolar iodinated contrast media) will delineate three physiological narrowings of the esophagus. The first narrowing is the normal upper esophageal

Figure 1.11 Intermittent minimal aspiration during swallowing in a normal newborn. Single frame from a digital video loop.

sphincter. In infants the contraction of lower constrictor pharyngeal muscle can simulate a true esophageal stenosis. However, this is only a transient functional disturbance in young children, which disappears spontaneously with increasing age. The second narrowing is the crossing of the aortic arch and the adjacent left main stem bronchus with the mid-portion of the esophagus. The third narrowing of the esophagus is the lower esophageal sphincter, i.e. cardia. These narrowings are important in foreign-body ingestion. The pressure zone in the lower esophageal sphincter is not fully developed in infants up to the age of six to eight months. This can result in gastroesophageal reflux. Similarly, the fixation of the esophagus in the hiatus of the diaphragm is not very tight, which can result in a slight gliding of the cardia. However this finding should not be interpreted as hiatus hernia, because it can disappear with further growth. The peristalsis of the esophagus is not fully developed in the first six months. Although the fast longitudinal contraction of the proximal third of the esophagus is well developed in the newborn, there are various abnormalities of the other parts often visible in healthy infants:

1. The entire esophagus may be intermittently wide and atonic.
2. Strong circumferential contractions may be intermittently visible in the mid-portion.
3. Jo-Jo peristalsis of the entire esophagus may be seen.
4. A hypertonic cardia may cause delayed passage in the distal esophagus.

All of these functional abnormalities gradually disappear by the end of the first year. Gastric emptying is a complex process of concurrent actions and can be influenced by extrinsic and intrinsic factors. The position of the stomach is related to the position of the atria of the heart. The normal anatomy is concordant between the left-sided heart (left atrium), left-sided stomach and left bilobed lung. In situs inversus, there is a mirror-image situation. In heterotaxia syndromes, the situation is disconcordant; e.g. the heart can be left sided, but the stomach is on the right side with many associated abnormalities which are beyond the scope of this chapter.

The duodenum and the small bowel rotate several times with subsequent fixation of the bowel at the posterior abdominal wall. The normal duodenojejunal junction is located to the left of the spine and at the level of the pyloric canal (Figure 1.12). This important landmark is connected with the hiatus oesophagei via the Treitz' ligament. The small bowel mesentery runs from the duodenojejunal junction in the left upper abdominal quadrant, in an oblique and caudal direction to the right iliac fossa (RIF), where it ends at the right-sided colon with the free cecum and appendix. Consequently, the jejunum is located in the left upper abdomen, and the ileum in the right lower part of the abdomen. The main bowel artery is the superior mesenteric artery which is normally to the left of the superior mesenteric vein. In most patients with malrotation, this anatomical situation is reversed. However, exceptions occur. The evaluation of the normal position of the duodenojejunal junction via an upper GI study is considered a more reliable indicator for exclusion of a malrotation than evaluation of the position of the cecum via an enema. The neonatal colon has a small lumen and typically no haustra. The position of the cecum in the young infant is higher than in adults and in most cases in the mid-position between the right colonic flexure (Figure 1.13) and its future final position in the right lower quadrant. The lengths of the sigmoid colon and of both colonic flexures are very variable. The rectum is often dilated compared to other parts of the large bowel. Haustra of the large bowel are observed at three to six months after birth.

The baby swallows air even in the birth canal, i.e. before the first cry and first breath. Air in the stomach rapidly passes the pylorus and the small bowel. Intraluminal air has reached

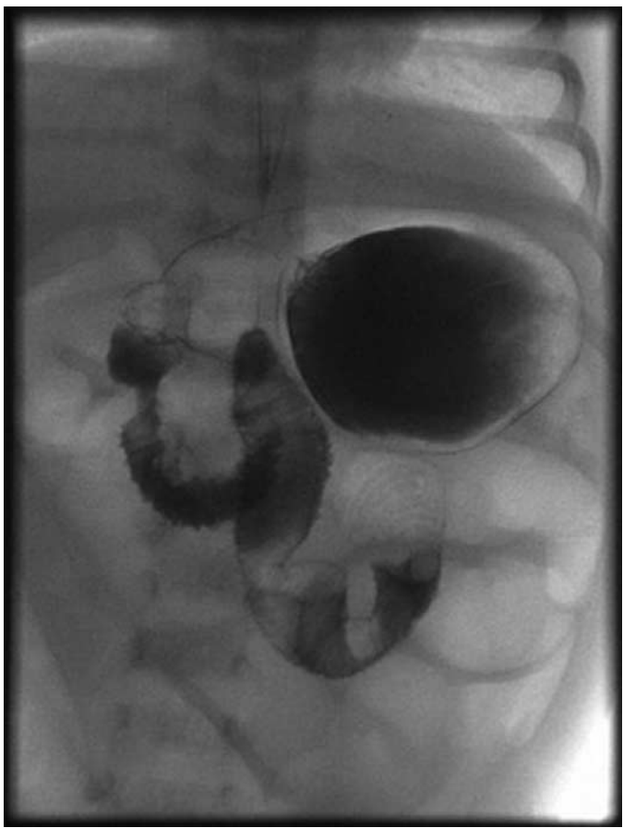

Figure 1.12 Normal stomach and duodenum in an infant.

the colon after 4–8 hours, and the rectum after 12–24 hours. Concurrently with the progress of bowel air, the newborn will pass the meconium. In premature babies the air and meconium passage is often delayed.

In infants, air is noted in all bowel loops, including the rectum. In older children, the stomach and small bowel are filled with various amounts of swallowed air, while there is little gas and stool in the large bowel. Some otherwise normal children swallow air all the time and may have a large air-filled stomach and a lot of air in the whole bowel. This is called aerophagia. This is a self-limited and transitory phenomenon and must be differentiated from meteorism and bowel obstruction of any cause.

Kidney and ureters

The main diagnostic procedures are sonography and renal scintigraphy with ^{99m}Tc MAG3 (technetium 99m mercaptyl-acetyltriglycine). The normal proximal and juxtavesical segments of the ureter can be sonographically visualized in the well-hydrated child with a full bladder. However, even markedly dilated ureters can be missed with ultrasound when a lot of bowel air/gas is present. In some patients, ^{99m}Tc DMSA (technetium 99m-labeled dimercaptosuccinic acid) is indicated, e.g. to evaluate the functional renal cortex, e.g. in

Figure 1.13 Normal colon in a newborn.

pyelonephritis. MR is helpful in evaluation of obstructive uropathies, and crucial for the comprehensive diagnosis of complex genitourinary malformations. Doppler sonography and MR angiography are useful for the evaluation of renal vessel abnormalities. Forty percent of normal patients with normal kidneys have more than one renal artery. Low dose CT is the method of choice in suspected urolithiasis.

The kidneys develop from seven ventral and seven dorsal renculi. A renculus is the smallest anatomical element which is composed of a cortical cap, a medullar pyramid, a calyx and surrounding blood vessels. The newborn kidney has a typical lobulated surface caused by the incomplete fusion of the renculi. During renal growth, the fusion of the renculi progresses continuously. The smoothing of the surface of the upper and lower poles of the kidney starts between year one and two of age. The fusion is incomplete at two sites, ventro-medially at the upper pole of the right kidney, and dorsally in the mid-portion of both kidneys. This finding has been described by F. Hoffer as the interrenicular junction (Figure 1.14).

In many infants during the first year, the renal cortex is narrow and hyperechoic compared to the liver parenchyma on US (Table 1.2). The triangular medullar pyramids at this age are large, compared to the overlying cortex, and extremely hypoechoic. Starting at the age of six months, the echogenicity of the renal cortex decreases gradually. Beyond infancy the cortex is hypoechoic compared to the liver. The renal sinus becomes enlarged by the deposition of fat, which begins at about six to eight years and progresses during puberty, reaching